Environmental Research Letters

LETTER • **OPEN ACCESS**

Simulated sensitivity of African terrestrial ecosystem photosynthesis to rainfall frequency, intensity, and rainy season length

Environmental Research Letters

LETTER

Simulated sensitivity of African terrestrial ecosystem photosynthesis to rainfall frequency, intensity, and rainy season length

Kaiyu Guan[1,12], Stephen P Good[2], Kelly K Caylor[3], David Medvigy[4], Ming Pan[5], Eric F Wood[5], Hisashi Sato[6], Michela Biasutti[7], Min Chen[8], Anders Ahlström[9,11] and Xiangtao Xu[10]

1 Department of Natural Resources and Environmental Sciences and National Center for Supercomputing Applications, University of Illinois at Urbana-Champaign, Urbana, IL 61801, United States of America
2 Department of Biological and Ecological Engineering, Oregon State University, Corvallis, OR 97331, United States of America
3 Department of Geography, Bren School of Environmental Science & Management, University of California - Santa Barbara, Santa Barbara, CA 93106, United States of America
4 Department of Biological Sciences, University of Notre Dame, Notre Dame, IN 46556, United States of America
5 Department of Civil and Environmental Engineering, Princeton University, Princeton, NJ 08544, United States of America
6 Institute of Arctic Climate and Environment Research, Japan Agency for Marine-Earth Science and Technology (JAMSTEC), 3173-25 Showamachi, Kanazawa-ku, Yokohama, 236-0001, Japan
7 Lamont-Doherty Earth Observatory of Columbia University, 61 Route 9 W, Palisades, NY, 10964-8000, United States of America
8 Joint Global Change Research Institute, Pacific Northwest National Laboratory, College Park, MD, United States of America
9 Department of Earth System Science, Stanford University, Stanford, CA 94025, United States of America
10 Department of Organismic and Evolutionary Biology, Harvard University, Cambridge, MA 02138, United States of America
11 Department of Physical Geography and Ecosystem Science, Lund University, 223 62 Lund, Sweden
12 Author to whom any correspondence should be addressed.

E-mail: kaiyug@illinois.edu

Keywords: Africa, water stress, rainfall frequency, rainfall intensity, rainy season length, dynamic vegetation modeling

Supplementary material for this article is available online

OPEN ACCESS

RECEIVED
2 September 2017

REVISED
29 November 2017

ACCEPTED FOR PUBLICATION
5 December 2017

PUBLISHED
16 February 2018

Abstract

There is growing evidence of ongoing changes in the statistics of intra-seasonal rainfall variability over large parts of the world. Changes in annual total rainfall may arise from shifts, either singly or in a combination, of distinctive intra-seasonal characteristics –i.e. rainfall frequency, rainfall intensity, and rainfall seasonality. Understanding how various ecosystems respond to the changes in intra-seasonal rainfall characteristics is critical for predictions of future biome shifts and ecosystem services under climate change, especially for arid and semi-arid ecosystems. Here, we use an advanced dynamic vegetation model (SEIB-DGVM) coupled with a stochastic rainfall/weather simulator to answer the following question: how does the productivity of ecosystems respond to a given percentage change in the total seasonal rainfall that is realized by varying only one of the three rainfall characteristics (rainfall frequency, intensity, and rainy season length)? We conducted ensemble simulations for continental Africa for a realistic range of changes (−20% ∼ +20%) in total rainfall amount. We find that the simulated ecosystem productivity (measured by gross primary production, GPP) shows distinctive responses to the intra-seasonal rainfall characteristics. Specifically, increase in rainfall frequency can lead to 28% more GPP increase than the same percentage increase in rainfall intensity; in tropical woodlands, GPP sensitivity to changes in rainy season length is ∼4 times larger than to the same percentage changes in rainfall frequency or intensity. In contrast, shifts in the simulated biome distribution are much less sensitive to intra-seasonal rainfall characteristics than they are to total rainfall amount. Our results reveal three major distinctive productivity responses to seasonal rainfall variability—'chronic water stress', 'acute water stress' and 'minimum water stress' - which are respectively associated with three broad spatial patterns of African ecosystem physiognomy, i.e. savannas, woodlands, and tropical forests.

1. Introduction

Understanding climate-ecosystem interactions requires not only the consideration of the mean state of climate (e.g. mean temperature and mean annual rainfall), but also of the intra-seasonal and inter-annual variability of meteorological drivers (Easterling 2000, Knapp *et al* 2002, Medvigy *et al* 2010, Good and Caylor 2011, Guan *et al* 2014a). For a single rainy season, the total seasonal rainfall can be conceptually characterized through three distinctive intra-seasonal characteristics at daily scale: rainfall frequency during the rainy season λ (day^{-1}), rainfall intensity during the rainy season α (mm), and rainy season length T_w (days). Significant spatial heterogeneity exists in these rainfall characteristics across Africa (figure 1). The product of these three rainfall characteristics determines the total amount of rainfall during the rainy season (Rodrigue-Iturbe 1984), and their variations influence the variability of rainfall at seasonal (Rodriguez-Iturbe and Porporato 2004) and inter-annual time scales (Franz *et al* 2010, Good *et al* 2016). Climate change causes complex changes in these intra-seasonal rainfall characteristics and shifts both the mean and the variability of rainfall in concert (Medvigy and Beaulieu 2012, Feng *et al* 2013, Easterling 2000). More intense and less frequent rainfall has been observed and projected globally (Trenberth *et al* 2003, Giorgi *et al* 2011, Pascale *et al* 2016), and possible shifts in rainfall seasonality are expected for tropical regions (Seth *et al* 2013, Chou *et al* 2013, Duffy *et al* 2015). Africa, which includes one third of the global dry and semi-dry ecosystems, may be particular sensitive to changes in these rainfall characteristics (Good and Caylor 2011, Guan *et al* 2014a). Increased rainfall intensity and decreased rainfall frequency have already been observed in central Kenya (Franz *et al* 2010) and West Africa (Lodoun *et al* 2013, Panthou *et al* 2014), while the shortening and the shift of the rainy season have been projected for the Sahel (Biasutti and Sobel 2009) and Southern Africa (Shongwe *et al* 2009). Understanding the ecological implications of these changes in rainfall characteristics is necessary to increase the resilience and adaptability of our society and to maintain the ecosystem services that, directly or indirectly, support the livelihood and wellbeing of billions of humans.

Variations in different rainfall statistics (λ, α, T_w) can impose distinctive types of water stress on terrestrial ecosystems. Rainfall frequency and rainfall intensity affect ecosystem function and structure primarily within the rainy season—mostly through their influence on short-term soil moisture dynamics (Porporato *et al* 2004). Except for extremely dry regions (Thomey *et al* 2011), increased rainfall frequency with constant seasonal rainfall totals usually increases plant growth by shortening the time that root-zone soil moisture drops below critical thresholds (e.g. the wilting point) (Daly *et al* 2004, Good and Caylor 2011). Different from rainfall frequency or intensity, rainy season length exerts an ecological influence through defining a temporal niche during which favorable conditions of soil water supply for plant growth are met. During the dry season, the lack of available soil water forces dormancy or termination for most plant physiological and metabolic activities. Rainy/dry season length can further affect fire season and fuel load, and possibly impose extra constraints on ecosystem structure and dynamics (Archibald *et al* 2009, Sankaran *et al* 2005, Lehmann *et al* 2014, Bond *et al* 2005). Thus the impacts from changes in intra-seasonal rainfall characteristics are likely to differ across ecosystems (Weltzin *et al* 2003, Good and Caylor 2011). Given the above complexities, analyses of rainfall-related ecosystem changes commonly use seasonal total rainfall amount as a single explanatory variable (e.g. Sankaran *et al* 2005), thus neglecting all the intra-seasonal rainfall variabilities. Those studies that consider intra-seasonal rainfall variability usually only focus on a specific type of rainfall characteristics (e.g. Ross *et al* 2012), without capturing the full spectrum of variability. A study that considers a comprehensive set of intra-seasonal rainfall characteristics and quantifies their impacts across ecosystems is thus needed to better understand ecosystem-climate interactions and to predict ecosystem biogeography under climate change.

Various approaches have been used to study the impact of intra-seasonal rainfall characteristics on ecosystem structure and function. Field-based rainfall manipulation experiments are widely popular (Heisler-White *et al* 2009, Kulmatiski and Beard 2013, Knapp *et al* 2002), but such experiments often explore one or two extreme rainfall scenarios for a certain ecosystem (mostly dryland savanna or grassland) and can be challenging to expand to other ecosystems. Another approach is to infer empirical relationships from large datasets (e.g. ecosystem properties, climate data, fire regimes) (Good and Caylor 2011, Sankaran *et al* 2005, Staver *et al* 2011, Lehmann *et al* 2014, Xu *et al* 2018). While these data-driven empirical syntheses have generated rich knowledge, they are inappropriate to test 'what if' questions for out-of-sample hypothetical scenarios. The last approach is to use the analytical (Rohr *et al* 2013, Schaffer *et al* 2015) or process-based simulation models (Xu *et al* 2015, Fernandez-Illescas and Rodriguez-Iturbe 2003, Guan *et al* 2014a) to make theoretical predictions. Over large regions across various ecosystems, models that have been properly validated can provide a useful tool for both diagnostic and prognostic purposes.

Here we use a modeling framework to quantitatively assess ecosystem sensitivities to individual shifts of rainfall characteristics (rainfall frequency, intensity, and rainy season length) at a broad spatial scale. The widespread distribution of water-limited ecosystems in Africa has made this continent an ideal area to explore the range of sensitivities to rainfall characteristics. We present a series of experiments which use an

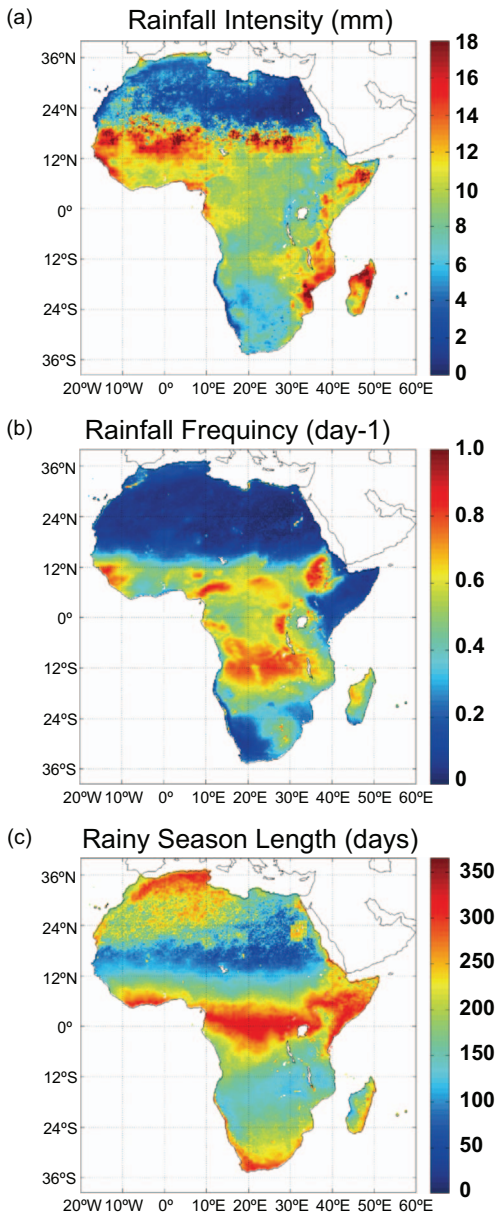

Figure 1. Intra-seasonal rainfall characteristics of the Africa continent for daily rainfall. The statistics are derived from the TRMM 3b42V7 product at its original resolution of 0.25° by 0.25° from 1998–2002. The rainy day threshold is 0 mm day^{-1}. (*a*) Average rainfall intensity during rainy season (mm); (*b*) average rainfall frequency during rainy season (day^{-1}); (*c*) average rainy season length (days). Rainy season is defined as the period that includes 90% of the total annual precipitation, and it varies from year to year.

advanced dynamic vegetation model (SEIB-DGVM) that has been independently validated in the African continent (Sato and Ise 2012), and a stochastic rainfall model and weather generator. The central questions we address are: (1) how do different African biomes respond to shifts in the three key intra-seasonal rainfall characteristics? (2) What are the implications of these diverse ecosystem responses in the context of projected climate change?

2. Methods and materials

2.1. Overview of the methods

Our modeling framework quantifies the sensitivity of simulated ecosystem photosynthesis (as measured by gross primary productivity, GPP) and biome geographic distributions to small perturbations in one of the three rainfall characteristics, while the other two are fixed to their current climatological values. We assume that GPP is a function of rainfall intensity (α), rainfall frequency (λ) and rainy season length (T_w), i.e. $\mathrm{GPP} = \mathrm{G}\left(\alpha, \lambda, T_w\right)$. Following Rodriguez-Iturbe and Porporato (2004) and Guan *et al* (2014a), we assume there is only a single rainy season with negligible dry season rainfall, which is the case for 92% of all the vegetated area in the Africa continent. The detailed mathematical derivation of the stochastic rainfall characteristics and their implementation within the weather generator are provided in section 2.3.

We design the following sensitivity experiments (table 1). We vary one at a time of the three

Table 1. Experiment designs. 'Obs' refers that the rainfall is purely from the observation, 'Syn' refers that the rainfall forcing is synthetically generated based on the climatology of the corresponding rainfall characteristics. '±20%,±10%' means that we perturb a specific rainfall characteristic to increase/decrease 20% and 10% away from the current climatology value and then use the weather generator to create realistic rainfall and other climate forcings. The total rainfall amount changes by '±18%,±9%' as we assume only rainy season that covers 90% of the total annual rainfall (see details in section 2.3).

Experiment number	Mean climate	Rainfall characteristics			Purpose
	P	α	λ	T_w	
$S_{climatology}$	Obs	Obs	Obs	Obs	Climatology run
$S_{control}$	Syn	Syn	Syn	Syn	Control run
Exp 1(S_α)	±18%,±9%	±20%,±10%	Syn	Syn	To calculate $\frac{\partial GPP/GPP}{\partial\alpha/\alpha}$
Exp 2(S_λ)	±18%,±9%	Syn	±20%,±10%	Syn	To calculate $\frac{\partial GPP/GPP}{\partial\lambda/\lambda}$
Exp 3(S_{Tw})	±18%,±9%	Syn	Syn	±20%,±10%	To calculate $\frac{\partial GPP/GPP}{\partial T_w/T_w}$

rainfall characteristics at four percentage change levels (−20%, −10%, +10% and +20%) from the current climatological state, while fixing the other two rainfall characteristics at their current climatological values. For each rainfall scenario, we generate six 500-year rainfall realizations (i.e. ensemble members) to account for the stochasticity of the synthetic rainfall model. These six rainfall realizations, with their corresponding climate variables, are used to drive the SEIB-DGVM from which the ensemble mean annual GPP is calculated and normalized by the annual mean GPP from the control run. Adjusting the change over the five percentage scenarios (−20%, −10%, 0%-control run, +10% and +20%) allows us to assess whether the derived GPP sensitivities are linear within the perturbation range. We find that these GPP sensitivities can be mostly treated as linear except for the tropical forests, which show a slight non-linearity (figure S5) but this non-linearity has minimal impact on our results and conclusion. The results shown in the main text are the GPP sensitivity derived from the −10% and +10% scenarios. Since we only apply small perturbations in the rainfall characteristics and assume $GPP = G(\alpha, \lambda, T_w)$, in the results we will analyze the relative changes in GPP normalized by the perturbation of each rainfall characteristics, i.e. $\frac{\partial GPP/GPP}{\partial\alpha/\alpha}$, $\frac{\partial GPP/GPP}{\partial\lambda/\lambda}$, and $\frac{\partial GPP/GPP}{\partial T_w/T_w}$, which will be unitless.

2.2. SEIB-DGVM dynamic vegetation model

We use the well-validated dynamic vegetation model SEIB-DGVM (Sato and Ise 2012). This model explicitly simulates the dynamics of fine-scale ecosystem structure and function for a set of virtual vegetation patches to represent large-scale ecosystem features. Individual plants are simulated from establishment, through growth, and resource competition with other plants, and finally to senescence, in order to create gaps in which recruitment of plants can occur. The SEIB-DGVM includes mechanistically-based and empirically-based algorithms for land physical processes, plant physiological processes, and plant competition processes (Sato and Ise 2012).

Specifically, the soil hydrology follows Sato *et al* (2010), which assumes that soil water is retained as if it were in a bucket and is only lost when it exceeds a maximum volume. The model divides soil column into layers, each of 10 cm in depth, and liquid water in the soil fills from the deep soil layers until it reaches field capacity. The model assumes no bottom drainage, and hence runoff can only occurs as surface runoff when all soil layers are saturated with water. The 'effective' bucket depth is determined by the number of the layers from which evapotranspiration occurs: it is assumed to be the top five layers of the soil column. With this scheme, the model was calibrated to reconstruct annual GPP, biomass, and runoff averaged over the African continent. After this calibration, the model reasonably reconstructs geographical distributions of biomass, plant productivity, and biome (Sato and Ise 2012). It is worth noting that SEIB-DGVM only simulates saturation-excess runoff, but not infiltration-excess runoff. Considering SEIB-DGVM functions at the daily step, and infiltration-excess runoff happens at much shorter time scales, it is reasonable to only consider saturation-excess runoff process at the daily scale here.

SEIB-DGVM uses a representation of plant water stress based on soil moisture status ($stat_{water}$), as $stat_{water} = (S - S_w)/(S_f - S_w)$, where S, S_w, and S_f refer to the fraction of volumetric soil water content within the rooting depth, at the wilting point, and at field capacity, respectively. A water stress factor (w) is then calculated as $w = 2 \times stat_{water} - stat_{water}^2$, where the quadratic term is included to capture the non-linear response of plant water stress to soil moisture (Sato and Ise 2012, Ronda *et al* 2001), and this water stress factor directly acts to scale the stomatal conductance for plant transpiration and carbon assimilation. For simplicity, all the soil-dependent parameters are derived from soil properties from Global Soil Wetness Project 2 (GSWP2, http://cola.gmu.edu/gswp/).

The model includes two tropical woody plant functional types (PFTs) and two grass PFTs. Specifically the two tropical woody PFTs were developed in the model based on the hydroclimatic conditions: (1) 'tropical evergreen trees' which only develop where water resources are sufficient all year around, so they can maintain leaves for all seasons; (2) 'tropical deciduous trees' which develop where dry and wet seasons both exist and only the wet season can provide enough to fulfill plant water needs, and the trees shed leaves

during dry seasons to avoid water stress (figure S3) (Sato and Ise 2012). Furthermore, $stat_{water}$ also controls leaf phenology in the tropical deciduous tree PFT through an empirically delivered time parameter, D_{max}. When the D_{max} day running average of $stat_{water}$ exceeds 0.0, the phase changes from dormant to growth, whereas when the D_{max} day running average of $stat_{water}$ falls below 0.0, the phase changes from growth into a dormant phase. D_{max} was calibrated to 10 d. SEIB-DGVM simulates two grass PFTs, i.e. C_3 or C_4 grass, depending on the environments. In tropical Africa C_4 grass usually dominates.

The SEIB-DGVM is run at one-degree spatial resolution and at a daily step. Although the spatial and temporal resolutions of the SEIB-DGVM are coarse, the model reasonably reconstructs geographical patterns of biomass, plant productivity, and biome type along the known aridity gradients for the African continent (Sato and Ise 2012), and thereby it is appropriate for this analysis. It is spun-up for 2000 years, during which it is driven by the observed climate (1970−2000) repeatedly to allow the soil carbon pool to reach steady state and then followed by a 500 year simulation driven by a specific rainfall scenario so that the biome distribution reaches to a new steady state.

To understand the direct impacts of intra-seasonal rainfall variability, we turn off the fire component of the SEIB-DGVM to exclude the effects of fire-mediated feedbacks. It is worth noting that though we did not simulate fire in the current work, the SEIB-DVGM was calibrated with allowance of wild fire. Actually, a fire suppression simulation of the SEIB-DGVM indicated that fire is required for reconstructing savanna ecosystems in some areas of Africa: without wildfire in these regions, it reconstructs forest ecosystems instead of savanna (Sato and Ise 2012). Though we are aware of the important role of fire in interacting with rainfall seasonality and in influencing Africa ecosystems (Archibald *et al* 2009, Bond *et al* 2005), we aim to focus our scenarios on the pure impact of rainfall characteristics and leave the study of the fire-rainfall interaction to other future work. For similar reasons, we fix the atmospheric CO_2 concentration at 380 ppmv to exclude possible impacts of CO_2 fertilization effects.

2.3. Stochastic rainfall model and the weather generator

Our stochastic rainfall model is based on the marked Poisson process (Rodriguez-Iturbe and Porporato 2004, Guan *et al* 2014a). A rainy day is defined when the daily rainfall amount is more than 0 mm. Since SEIB-DGVM runs at the daily step, we do not consider sub-daily rainfall events, and a rainy day is treated as a rainy event. Rainfall intensity is only defined for rainy days, thus it has the unit of mm. The arrival of rainfall events is a Poisson process, i.e. the distribution of time between rainfall events is exponential with mean $1/\lambda$, and λ is estimated as the mean of rainfall frequency (unit: 1/day): $f_t(t) = \lambda e^{-\lambda t}$, for $t \geq 0$ (with t as the time between events). The depth of rainfall events (i.e. rainfall intensity) is exponentially distributed with mean α, and α is estimated as the mean of rainfall depth only from the rainy days (mm): $f_H(h) = \frac{1}{\alpha} e^{-\frac{1}{\alpha}h}$, for $h \geq 0$ (with h as the dummy variable). The wet season length T_w is modeled as a beta distribution bounded from 0 to 1, scaled by 365 d. Thus the cumulative total rainfall for a certain period T_i has the mean of $E[\lambda_i]E[\alpha_i]E[T_i]$ (mm), with subscript i referring to a specific period, and E[x] referring to the statistical mean of the random variable x.

The mean annual precipitation (MAP) can be expressed as $MAP = E[\lambda]\ E[\alpha]\ E[T_w] / f_w$, where f_w is the fraction of the MAP that occurs during the rainy season. In our model, we set f_w to be 0.9, resulting in the 'rainy (or wet) season' being the period that includes 90% of total annual rainfall, and 'dry season' contains the rest 10% of MAP. The starting/ending dates of the 'wet season' are determined in a more complex way than has been detailed in Guan *et al* (2015). Here, when generating a synthetic rainfall time series, we first randomly generate T_w using the beta distribution with derived parameters from the observation data (see below), and then simulate 'wet season' and 'dry season' rainfall respectively using two marked Poisson processes with specific derived parameters. We estimate all the rainfall parameters (including the mean and variance of rainfall frequency, intensity and length of wet and dry seasons) for the African continent from the satellite-gauge-merged rainfall measurement from Tropical Rainfall Measuring Mission (TRMM) 3b42−V7 daily rainfall product (Huffman *et al* 2007) for the period from 1998–2012. We derive these rainfall model parameters at the spatial resolution of the TRMM data (i.e. 0.25 degree, figure 1), and then aggregate these parameters to 1 degree and finally generate grid-based synthetic rainfall time series for the continental Africa. It is cautionary that rainfall characteristics are sensitive to the spatial scale, as local-scale rainfall frequency is usually smaller than those derived from regional aggregated rainfall data (e.g. from satellite or climate models) (del Jesus *et al* 2015). However, because our dynamic vegetation model was calibrated using the rainfall inputs at the spatial resolution of 0.5–1 degree (Sato *et al* 2010, Sato and Ise 2012), we keep the consistency at this spatial scale and match TRMM-derived rainfall characteristics to the same scale. This stochastic rainfall model provides a convenient way to adjust rainfall patterns by varying one of the rainfall characteristics.

Other climate variables besides rainfall are necessary for driving the SEIB-DGVM. We build a weather generator by conditionally resampling from the historical records the necessary climat variables based on the simulated rainfall conditions. This method preserves the co-variations between rainfall and other climatic variables, as well as those among different

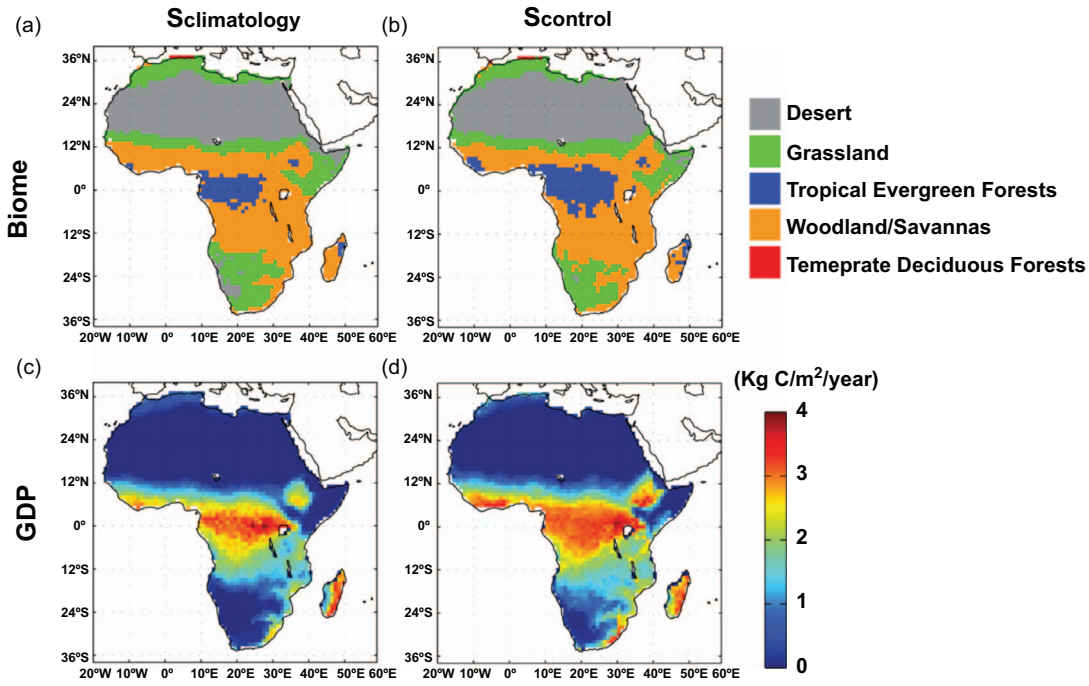

Figure 2. Comparison of simulated biomes and annual mean GPP using SEIB-DGVM in the $S_{climatology}$ and $S_{control}$ runs. The scatterplot between the two simulated GPP from the $S_{climatology}$ and $S_{control}$ runs are shown in figure S2.

climate variables. The resampled climate variables include air temperature, wind, and humidity from the Global Meteorological Forcing Dataset (Sheffield *et al* 2006), and cloud fraction and soil temperature from the Climate Forecast System Reanalysis from National Centers for Environmental Prediction (Saha *et al* 2010) (more details can be found in the supplementary materials available at stacks.iop.org/ERL/13/025013/mmedia).

3. Results and discussions

3.1. Validation of the SEIB-DGVM and the rainfall/weather generator

SEIB-DGVM has been widely validated for various ecosystems at global and regional scales (Sato and Ise 2012, Sato 2009, Sato *et al* 2010, 2007), and its simulations closely match ground and satellite observations of ecosystem composition, structure and function. Sato and Ise (2012) applied SEIB-DGVM to the whole African continent and found that this model can satisfactorily reproduce the spatial patterns of GPP and biomass measured from satellite remote sensing. Since the primary focus of the current work is GPP, we also compared GPP in the SEIB-DGVM simulation forced by the historical climate data (see details in 2.5) against the MODIS GPP for the Africa continent (figure S1) and found a high level of agreement that justifies the use of SEIB-DGVM for the current study.

To test the validity of the synthetic rainfall/weather generator, we run the SEIB-DGVM using the historical climate record ($S_{climatology}$) and the synthetic forcing ($S_{control}$), with the latter generated using the weather generator based on the rainfall characteristics derived from the former. Figure 2 shows that the SEIB-DGVM simulations driven by these two different forcings generate similar biome distributions with a Cohen's Kappa coefficient of 0.78 (Cohen 1960), and similar GPP patterns for Africa, with the linear fit of annual GPP as $GPP(S_{control}) = 1.03 \times GPP(S_{climatology}) + 0.215$ ($R^2 = 0.89$, $P < 0.0001$, figure S2). Biome and GPP patterns from both $S_{climatology}$ and $S_{control}$ are consistent with observations (Sato and Ise 2012). These results provide confidence in the appropriateness of using the synthetic weather generator to conduct our study.

3.2. Simulated biome sensitivity to intra-seasonal rainfall variability

We find that within the realistic range of changes ($-20\% \sim +20\%$) in total rainfall amount, the simulated change in biome distribution is mainly determined by the total rainfall amount rather than specific rainfall characteristics (figure 3, figure S4). This indicates that MAP is still the first-order determinant for biome distribution. However, there is non-negligible difference among the three rainfall characteristics, principal among these is that a change in T_w can lead to an increase in tropical evergreen forests as well as more tropical woodland expansion into grassland, compared with the same percentage changes in intensity or frequency. This finding has two important implications. First, it indicates that the distributions of tropical evergreen and deciduous trees are also sensitive to the shifts in wet season length (equivalently, the dry season length). Second, this finding also indicates that rainy

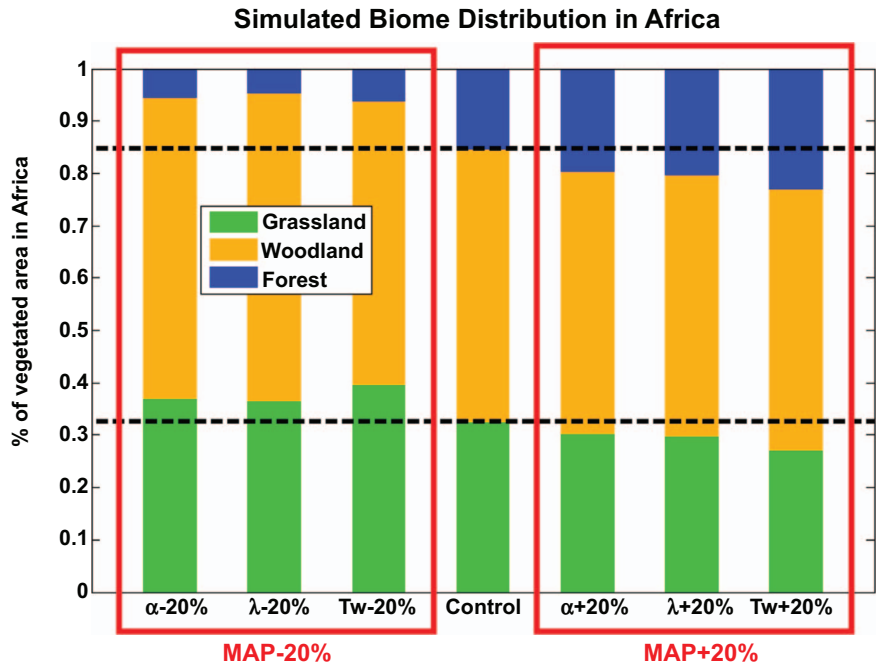

Figure 3. Simulated biome distribution under different rainfall change scenarios. The black dashed lines refer to the biome distribution from the 'control' run. The spatial patterns can be found in figure S4.

season length is also a major determinant of savanna structure (i.e. tree/grass fraction) and ecotone shifts.

3.3. Simulated GPP sensitivity to intra-seasonal rainfall variability

We find that the GPP sensitivities to rainfall intensity and frequency have similar spatial patterns and magnitudes (figures 4(*a*) and, (*c*)). Three distinct response regimes apparently arise as a function of mean annual precipitation (figures 4(*b*) and (*d*)). For regions with MAP below 700 mm year^{-1}, GPP has high positive sensitivity to both intensity and frequency ($\frac{\partial GPP/GPP}{\partial \alpha/\alpha}$ and $\frac{\partial GPP/GPP}{\partial \lambda/\lambda}$ >0.5, i.e. for a 10% increase in intensity or frequency, there would be more than a 5% increase in GPP). There is also a large variation (standard deviation ≈ 0.4) in the simulated GPP sensitivity. The peak sensitivities to both intensity and frequency happen at approximately 500 mm year^{-1}. In the MAP range from 700 to 1400 mm year^{-1}, GPP has much lower, but still positive, sensitivity (~0.1±0.05) to intensity and to frequency. A general trend of decreasing sensitivity is seen from 500 to 1400 mm year^{-1}, with the most dramatic decrease happening from 500 to 800 mm year^{-1}. When MAP is larger than 1400 mm year^{-1}, GPP shows slightly negative sensitivity to intensity and frequency. These results demonstrate that changes in intensity and frequency affect drylands the most, especially in regions with MAP below 700 mm year^{-1}—consistent with the existing ecohydrology literature about the importance of rainfall frequency and intensity in determining dryland soil moisture dynamics and plant productivity (Daly *et al* 2004, Rodriguez-Iturbe and Porporato 2004).

GPP sensitivity to T_w is systematically different than the sensitivity to intensity and frequency (figures 4(*e*) and (*f*)). The GPP sensitivity to T_w is high when MAP is below 700 mm year^{-1}, which is similarly to intensity and frequency. However, in the intermediate MAP range (700−1400 mm year^{-1}), changes in T_w would lead to three to four times larger changes in GPP than would result from the same percentage changes in intensity or frequency. The sensitivity of GPP to T_w significantly decreases at 1400−1600 mm year^{-1}and becomes almost zero when MAP is larger than 1600 mm year^{-1}.

Figure 5 further shows the scatterplots of GPP sensitivity to the three rainfall characteristics. Again, we find that GPP sensitivity to T_w is in general much larger than the GPP sensitivities to intensity (α) and to frequency (λ), with more than 93% of the grid cells showing higher $\frac{\partial GPP/GPP}{\partial Tw/Tw}$ than $\frac{\partial GPP/GPP}{\partial \alpha/\alpha}$ (i.e. above the 1:1 line in figure 5(*a*)), and more than 88% of the grids showing higher $\frac{\partial GPP/GPP}{\partial Tw/Tw}$ than $\frac{\partial GPP/GPP}{\partial \lambda/\lambda}$ (i.e. above the 1:1 line in figure 5(*b*)). Although the differences between the GPP sensitivities to frequency and intensity are subtle (figure 4), they are clearly identified in figure 5(*c*), which shows that the GPP sensitivity to intensity is only 78% of the GPP sensitivity to frequency.

3.4. A variability-based framework to study GPP-rainfall relationship

Based on the above results, we propose three types of vegetation responses to explain the different GPP sensitivities (figure 6). (1) In the low MAP regime (below 700 mm year^{-1}), ecosystem GPP would increase with MAP, regardless of whether the increase in MAP is

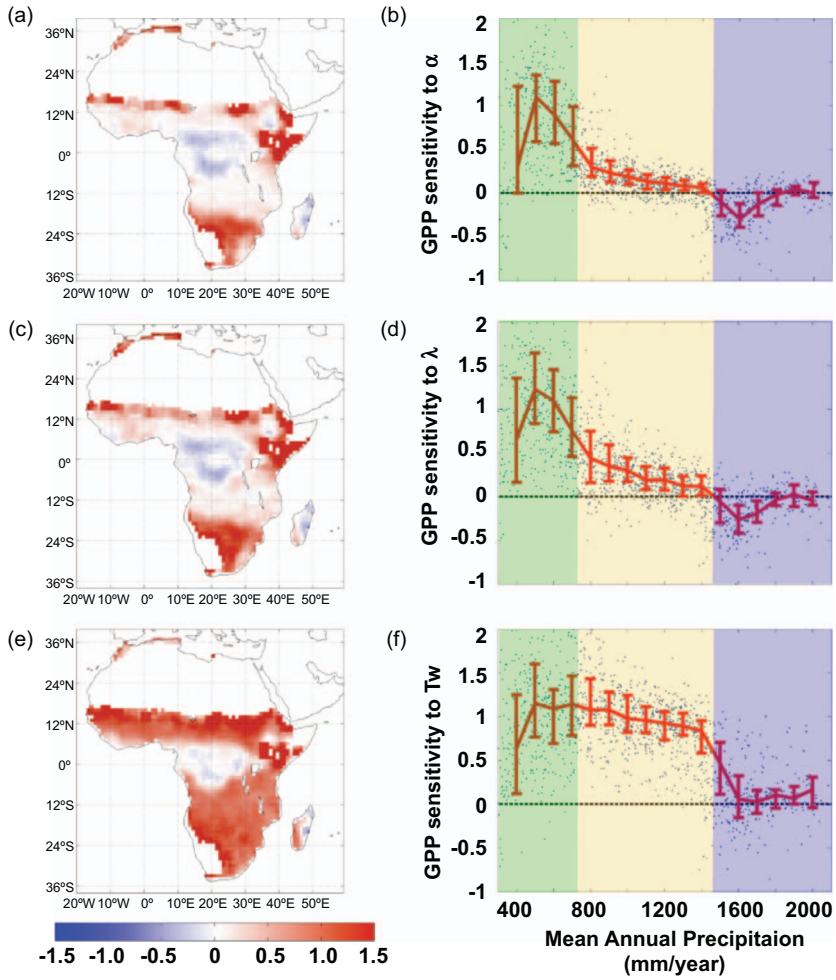

Figure 4. Relative GPP sensitivity to the three rainfall characteristics in Africa. The GPP sensitivity to rainfall intensity, frequency and T_w are shown in (*a*), (*c*) and (*e*) respectively. The colorshadings refer to the relative GPP change based on the annual mean GPP in the control run. For example, if the colorshading value is 1.0 in panel a, it means that if intensity increases 5% from the current state, the GPP will increase $1.0 \times GPP_{control} \times 5\%$, assuming the linearity of the sensitivity within the small perturbation (±10%). (*b*), (*d*) and (*f*) show the GPP sensitivity to the three rainfall characteristics as a function of MAP. The solid line refers to the median, the errorbars indicate 25% and 75% quantile values, and each bin is 100 mm year^{-1}. The three colorshades (red, green and blue) in right column correspond to the low (<700 mm year^{-1}), intermediate (700–1500 mm year^{-1}), and high (>1500 mm year^{-1}) MAP range, respectively.

achieved by increasing rainfall intensity, or rainfall frequency, or the length of the rainy season. Vegetation in this MAP regime experiences water scarcity in both the wet seasons (i.e. $\frac{\partial GPP/GPP}{\partial \alpha/\alpha} > 0.5$, $\frac{\partial GPP/GPP}{\partial \lambda/\lambda} > 0.5$) and dry seasons (i.e. $\frac{\partial GPP/GPP}{\partial T_w/T_w} > 0.5$), we describe this sensitivity as the 'chronic water stress' response. (2) For plants in the intermediate MAP range (700–1600 mm year^{-1}), GPP is largely insensitive to additional rainfall within the rainy season (from either intensity or frequency increases), because sufficient water is available during the rainy season (i.e. $\frac{\partial GPP/GPP}{\partial \alpha/\alpha}$ and $\frac{\partial GPP/GPP}{\partial \lambda/\lambda}$ range from [0, 0.3]); yet GPP is still highly sensitive to the changes in T_w (i.e. $\frac{\partial GPP/GPP}{\partial T_w/T_w} > 0.8$). Vegetation in this regime is mostly constrained by the length of the dry season, and we describe this sensitivity as 'acute water stress' response. (3) Finally, in the case of high MAP (above 1600 mm year^{-1}), vegetation has no sensitivity or sometimes a slightly negative sensitivity to increases in intensity or frequency within the rainy season, indicating little water stress. The slight negative sensitivity (i.e. $\frac{\partial GPP/GPP}{\partial \alpha/\alpha} < 0$, $\frac{\partial GPP/GPP}{\partial \lambda/\lambda} < 0$) likely arises from the correlation of rainfall and cloudiness. When rainfall amount is not a constraint, ecosystems are prone to radiation limitation instead; any increased cloudiness associated with more rain decreases incoming shortwave radiation and lowers potential ET demand. These regions are almost insensitive to the change in T_w (i.e. $\frac{\partial GPP/GPP}{\partial T_w/T_w} \cong 0$), mostly because their rainy season is close to the whole year and could not be further extended. We describe the sensitivity for this regime as 'minimum water stress' response.

We further construct a 'GPP sensitivity space' (figure 7) to synthesize our findings. The 'GPP sensitivity space' has its primary axis as the averaged GPP sensitivity to intensity and to frequency (these two are combined due to their similar responses in both magnitudes and spatial patterns) and its secondary axis

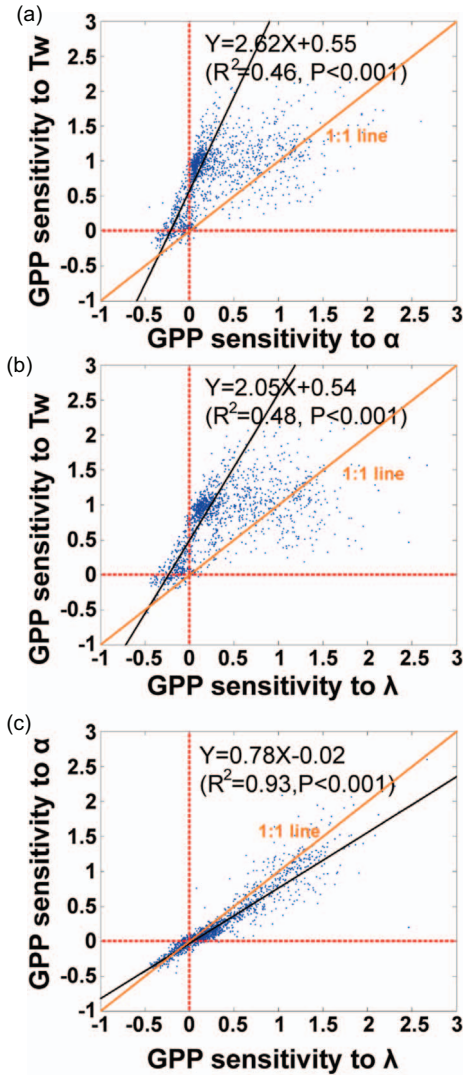

Figure 5. Scatterplot among the GPP sensitivities to the three rainfall characteristics. The orange line refers to 1:1 line, and black line refers to the linear fit.

as the GPP sensitivity to T_w. The three water stress regimes can be distinguished using the K-mean classification algorithm (Seber 1984), with the centroids of each type of water stresses shown in figure 7(*a*) and their boundaries delineated in figure 7(*b*). The 'minimum water stress' type has little sensitivity to T_w, and very small (and mostly negative) sensitivity to intensity and frequency. The 'acute water stress' type has large positive sensitivity to T_w, and very small (but positive) sensitivity to intensity and frequency. The 'chronic water stress' type has large positive sensitivity to increases in all the rainfall characteristics; this type has the largest variation. When spatially mapping back this GPP sensitivity space (figure 7(*b*)), we find that the spatial distribution of the clusters largely resembles the current distribution of biomes in Africa (figure 2), as the 'chronic water stress' type mostly overlaps with tropical grasslands, the 'acute water stress' type overlaps with tropical woodlands, and the 'minimum water stress' type is occupied by tropical forests.

We summarize that these biome-specific sensitivities to rainfall would be generated in the model primarily by PFT specific plant-physiological-properties. First, in savanna and grassland biomes, where the C4-type grass PFT dominates plant productivity, drought tolerance should be higher than in forest ecosystems. Second, while the grass PFT and the deciduous woody PFT can adjust their leafing days to changes in dry season length, the evergreen woody PFT has to maintain leafs even during the dry season, resulting in lower carbon uptake. The latter factor would primarily determine different responses of evergreen and deciduous forests to rain-days, because evergreen and deciduous woody PFTs shares identical stomatal conductance parameters in the model. It should be noted that changes in soil types would also affect these sensitivities, because soil parameters determine capacity of the "bucket" in the hydrology sub-model.

Areas with the 'acute water stress' response largely overlap with tropical woodlands (figure 2), and exhibits

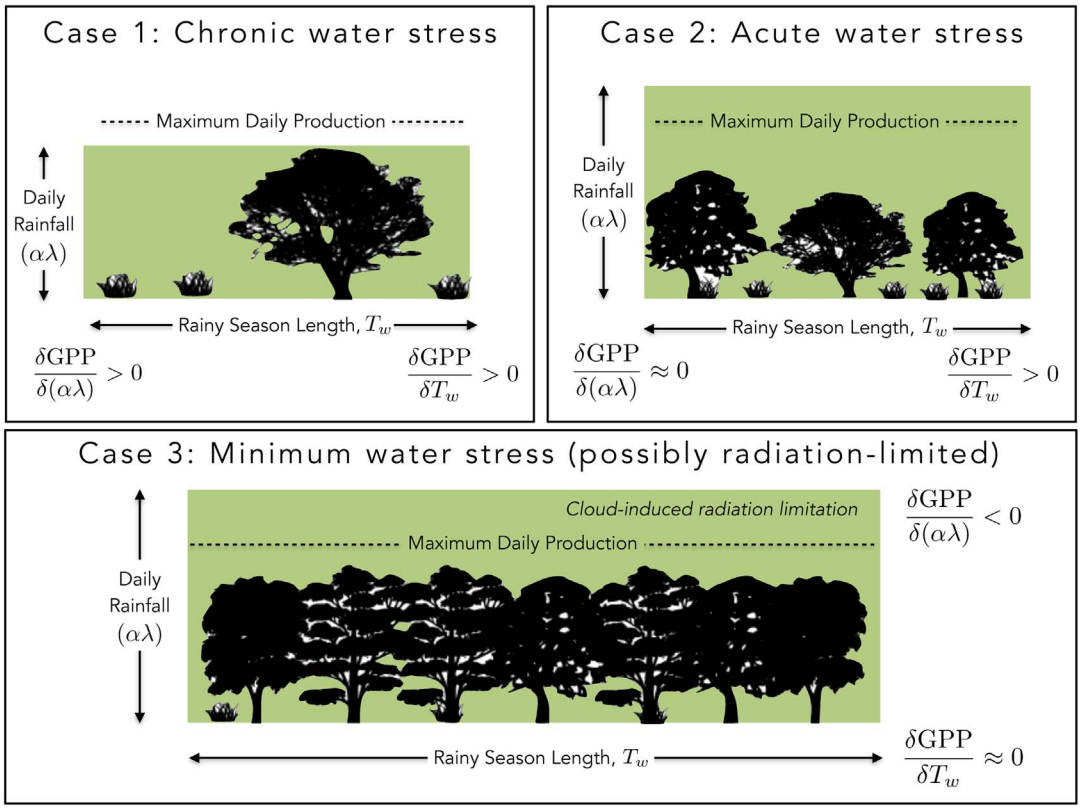

Figure 6. Conceptual explanation for biome-specific GPP sensitivity to the three rainfall characteristics. The green-box area conceptually indicate the amount of annual GPP.

little water stress during the rainy season. Both satellite-based (Huete *et al* 2002) and model-simulated productivity corroborate this finding (figure S6), and indicate that a majority of woodlands have similarly high maximum productivity during the growing season, regardless of widely different annual averaged values in productivity of the broad woodlands. In other words, most woodlands can achieve similarly high peak GPP, but their annual total GPP is largely constrained by the growing season length, which is tightly linked with T_w in tropical Africa (Guan *et al* 2014b). Though fire impacts have not been modeled in the current framework, we expect that feedbacks between fire occurrences and dry season length would further amplify the controls of dry season length on woodland productivity (Archibald *et al* 2009).

The GPP sensitivities to intensity and frequency (figures 4(*a*) and (*d*)) are similar, mostly because both intensity and frequency describe rainfall characteristics during the rainy season instead of dry season. Thus, only considering the ecological impacts from intensity or frequency cannot capture the effects arising from shifts in rainy season length. Nevertheless, there are still subtle differences between the effects of intensity and frequency, as shown by the fact that the GPP sensitivity to intensity is only 78% of the GPP sensitivity to frequency (figure 5(*c*)). Plants have little use for higher intensity (here, daily accumulation) if most of it ends up as runoff. Because SEIB-DGVM only considers 'saturation-excess runoff', here we envision the case in which daily rainfall and antecedent soil moisture are high, so that any newly added rainfall overfills the soil 'bucket' and produces saturation-excess runoff. This rainfall intensity impact should be differentiated from the mechanisms of 'infiltration-excess runoff'. The finding that tropical ecosystems in general have larger positive GPP sensitivity to frequency than to intensity is consistent with previous field and modeling studies suggesting that increases in rainfall frequency may be more beneficial to tropical ecosystems than increases in rainfall intensity, given the same change in total rainfall amount (Porporato *et al* 2004, Knapp *et al* 2002, Good and Caylor 2011).

3.5. Limitations of the current study

In the current study, we exclude the effects of fire and focus instead on the pure effect of rainfall, which is the first-order determinant for arid and semi-arid ecosystems (Strickland *et al* 2016, Lehmann *et al* 2014). We fully recognize the importance of fire, which has been found to strongly affect vegetation dynamics and composition for the savanna ecosystems (Dantas *et al* 2016, Bond *et al* 2005). Fire regime depends on both the soil moisture associated with rainfall scenarios and the fuel load associated with vegetation structure. This double dependency leads to a complex vegetation-fire-climate feedback (Lasslop *et al* 2016, Lehmann *et al* 2014), which has been challenging to model so far (Hantson *et al* 2016). Yet we have reasons to believe that our conclusions would largely hold even when considering

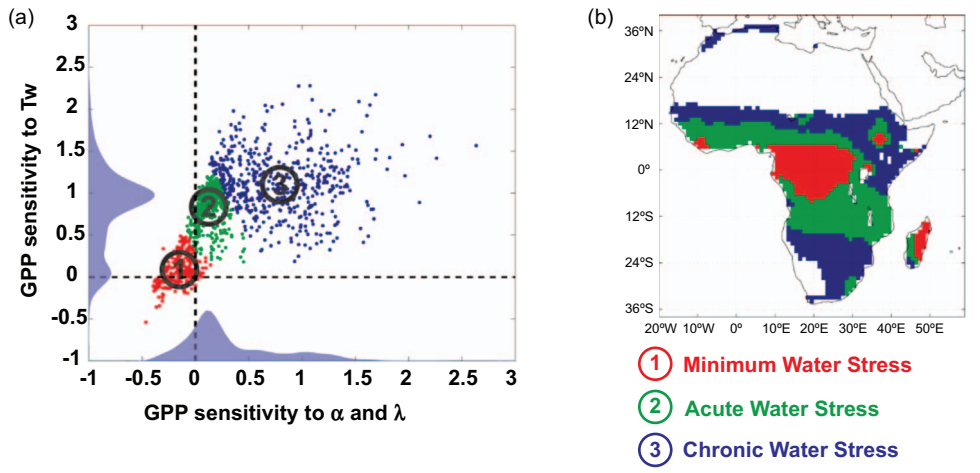

Figure 7. GPP sensitivity space and its spatial distribution. (*a*) The *x*-axis refers to the averaged GPP sensitivity to rainfall intensity and frequency, and the *y*-axis refers to the GPP sensitivity to T_w. The three-color scheme corresponds to 'Minimum Water Stress' (red), 'Acute Water Stress' (green), and 'Chronic Water Stress' (blue), with numbered circles locating in the centroid of each cluster derived from the K-mean classification (see section 3.4). The histograms of the GPP sensitivity are shown along the two axes. (*b*) Spatial pattern of the three clusters of GPP sensitivity to rainfall characteristics.

fire effects. First, fire effects would likely only influence the results for moist woodland or forest regions where rainfall is higher than 1000 mm (Staver *et al* 2011); fire is less of a concern for GPP in regions with chronic and acute water stress. Second, previous literature largely emphasized the fire impacts on the biome distribution, and the current study shows that intra-seasonal rainfall characteristics have little impact on the biome shifts. Therefore, this study can be regarded as an appropriate first estimate of the potential ecosystem response to changes in rainfall variability and we suggest that analysis of the interactions between fire and intra-season rainfall characteristics can be delayed to future studies.

This study relies on a single ecosystem model, with one way of modeling plant water stress (primarily through soil moisture) and vegetation dynamics. The simulated responses to the three intra-seasonal rainfall characteristics can be largely attributed to the parameterization of soil moisture stress on stomatal functioning. The spatial variations of the responses also arise from the heterogeneous rainfall patterns across space (figure 1) and the specific parameterizations of biophysical, phenological and biome determinations in SEIB-DGVM. The current study using SEIB-DGVM is a continental-scale modeling sensitivity analysis that demonstrates the importance of explicitly considering intra-seasonal rainfall characteristics. Thus, other models should confirm our results before the latter can inform climate change adaptation. Still, the relevant parametrizations in SEIB-DGVM are in line with the state-of-the-art in ecosystem models, and the model contains the necessary processes to be realistic.

Finally, we caution that our synthetic rainfall model is most suitable for the case of a single rainy season or a year-round rainy season (such as in the tropical forests). This covers 92% of the vegetated landscapes in Africa. The only exception is East Africa (i.e. Kenya, Ethiopia), which experiences two rainy seasons per year. Thus while we are confident in our results for the vast majority of the African continent, we are less confident for the East Africa region.

4. Conclusion

Not all rainfall regimes are ecologically the same: the same amount of change in rainfall, when effected through changes in rainfall frequency, intensity or seasonality, can lead to dramatically distinct responses across biomes. In particular, we find an amplified impact of changes in rainy season length on the GPP of tropical woodlands. The simulated range of GPP sensitivity to different rainfall statistics reflects the inherent sensitivity of different biomes to water stress. Our work emphasizes the necessity to incorporate high-frequency meteorological variability (Medvigy *et al* 2010) into the studies of climate-ecosystem interactions rather than considering only the time-mean climate drivers or a single type of change.

Acknowledgments

K Guan acknowledges financial support from the NASA New Investigator Award. K Guan and E F Wood jointly acknowledge support from the NASA NESSF Award. D Medvigy acknowledges support from the US Department of Energy, Office of Science, Office of Biological and Environmental Research, Terrestrial Ecosystem Science (TES) Program under award number DE-SC0014363. S P Good and K K Caylor acknowledge financial support from the National Science Foundation through the Grant EAR-0847368. M Biasutti acknowledges support from NSF-SES-10-48946.

ORCID iDs

Kaiyu Guan https://orcid.org/0000-0002-3499-6382

References

Archibald S, Roy D P, van Wilgen B W and Scholes R J 2009 What limits fire? An examination of drivers of burnt area in Southern Africa *Glob. Change Biol.* **15** 613–30

Biasutti M and Sobel A H 2009 Delayed Sahel rainfall and global seasonal cycle in a warmer climate *Geophys. Res. Lett.* **36** L23707

Bond W J, Woodward F I and Midgley G F 2005 The global distribution of ecosystems in a world without fire *New Phytol.* **165** 525–37

Chou C, Chiang J C H, Lan C-W, Chung C-H, Liao Y-C and Lee C-J 2013 Increase in the range between wet and dry season precipitation *Nat. Geosci.* **6** 263–7

Cohen J 1960 A coefficient of agreement for nominal scales *Educ. Psychol. Meas.* **20** 37–46

Daly E, Porporato A and Rodríguez-Iturbe I 2004 Coupled dynamics of photosynthesis, transpiration, and soil water balance. Part II: stochastic analysis and ecohydrological significance *J. Hydrometeorol.* **5** 559–66

Dantas V de L, Hirota M, Oliveira R S and Pausas J G 2016 Disturbance maintains alternative biome states *Ecol. Lett.* **19** 12–9

Duffy P B, Brando P, Asner G P and Field C B 2015 Projections of future meteorological drought and wet periods in the Amazon *Proc. Natl Acad. Sci.* **112** 13172–7

Easterling D R 2000 Climate extremes: observations, modeling, and impacts *Science* **289** 2068–74

Feng X, Porporato A and Rodriguez-Iturbe I 2013 Changes in rainfall seasonality in the tropics *Nat. Clim. Change* **3** 811–5

Fernandez-Illescas C P and Rodriguez-Iturbe I 2003 Hydrologically driven hierarchical competition–colonization models: the impact of interannual climate fluctuations *Ecol. Monogr.* **73** 207–22

Franz T E, Caylor K K, Nordbotten J M, Rodríguez-Iturbe I and Celia M a 2010 An ecohydrological approach to predicting regional woody species distribution patterns in dryland ecosystems *Adv. Water Resour.* **33** 215–30

Giorgi F, Im E-S, Coppola E, Diffenbaugh N S, Gao X J, Mariotti L and Shi Y 2011 Higher hydroclimatic intensity with global warming *J. Clim.* **24** 5309–24

Good S P and Caylor K K 2011 Climatological determinants of woody cover in Africa *Proc. Natl Acad. Sci. USA* **108** 4902–7

Good S P, Guan K and Caylor K K 2016 Global patterns of the contributions of storm frequency, intensity, and seasonality to interannual variability of precipitation *J. Clim.* **29** 3–15

Guan K, Good S P, Caylor K K, Sato H, Wood E F and Li H 2014a Continental-scale impacts of intra-seasonal rainfall variability on simulated ecosystem responses in Africa *Biogeosciences* **11** 6939–54

Guan K, Wood E F, Medvigy D, Kimball J, Pan M, Caylor K K, Sheffield J, Xu X and Jones M O 2014b Terrestrial hydrological controls on land surface phenology of African savannas and woodlands *J. Geophys. Res. Biogeosci.* **119** 1652–69

Guan K, Sultan B, Biasutti M, Baron C and Lobell D B 2015 What aspects of future rainfall changes matter for crop yields in West Africa? *Geophys. Res. Lett.* **42** 8001–10

Hantson S *et al* 2016 The status and challenge of global fire modelling *Biogeosciences* **13** 3359–75

Heisler-White J L, Blair J M, Kelly E F, Harmoney K and Knapp A K 2009 Contingent productivity responses to more extreme rainfall regimes across a grassland biome *Glob. Change Biol.* **15** 2894–904

Huete A, Didan K, Miura T, Rodriguez E P, Gao X and Ferreira L G 2002 Overview of the radiometric and biophysical performance of the MODIS vegetation indices *Remote Sens. Environ.* **83** 195–213

Huffman G J, Bolvin D T, Nelkin E J, Wolff D B, Adler R F, Gu G, Hong Y, Bowman K P and Stocker E F 2007 The TRMM multisatellite precipitation analysis (TMPA): quasi-global, multiyear, combined-sensor precipitation estimates at fine scales *J. Hydrometeorol.* **8** 38–55

del Jesus M, Rinaldo A and Rodríguez-Iturbe I 2015 Point rainfall statistics for ecohydrological analyses derived from satellite integrated rainfall measurements *Water Resour. Res.* **51** 2974–85

Knapp A K, Fay P A, Blair J M, Collins S L, Smith M D, Carlisle J D, Harper C W, Danner B T, Lett M S and McCarron J K 2002 Rainfall variability, carbon cycling, and plant species diversity in a mesic grassland *Science* **298** 2202–5

Kulmatiski A and Beard K H 2013 Woody plant encroachment facilitated by increased precipitation intensity *Nat. Clim. Change* **3** 833–7

Lasslop G, Brovkin V, Reick C H, Bathiany S and Kloster S 2016 Multiple stable states of tree cover in a global land surface model due to a fire-vegetation feedback *Geophys. Res. Lett.* **43** 6324–31

Lehmann C E R *et al* 2014 Savanna vegetation-fire-climate relationships differ among continents *Science* **343** 548–52

Lodoun T, Giannini A, Traoré P S, Somé L, Sanon M, Vaksmann M and Rasolodimby J M 2013 Changes in seasonal descriptors of precipitation in Burkina Faso associated with late 20th century drought and recovery in West Africa *Environ. Dev.* **5** 96–108

Medvigy D and Beaulieu C 2012 Trends in daily solar radiation and precipitation coefficients of variation since 1984 *J. Clim.* **25** 1330–9

Medvigy D, Wofsy S C, Munger J W and Moorcroft P R 2010 Responses of terrestrial ecosystems and carbon budgets to current and future environmental variability *Proc. Natl Acad. Sci. USA* **107** 8275–80

Panthou G, Vischel T and Lebel T 2014 Recent trends in the regime of extreme rainfall in the central Sahel *Int. J. Climatol.* **34** 3998–4006

Pascale S, Lucarini V, Feng X, Porporato A and Hasson S 2016 Projected changes of rainfall seasonality and dry spells in a high greenhouse gas emissions scenario *Clim. Dyn.* **46** 1331–50

Porporato A, Daly E and Rodriguez-Iturbe I 2004 Soil water balance and ecosystem response to climate change *Am. Nat.* **164** 625–32

Rodrigue-Iturbe I 1984 Scale considerations in the modeling of temporal rainfall *Water Resour. Res.* **20** 1611–9

Rodriguez-Iturbe I and Porporato A 2004 *Ecohydrology of Water-Controlled Ecosystems: Soil Moisture and Plant Dynamics* (Cambridge: Cambridge University Press)

Rohr T, Manzoni S, Feng X, Menezes R S C and Porporato A 2013 Effect of rainfall seasonality on carbon storage in tropical dry ecosystems *J. Geophys. Res. Biogeosci.* **118** 1156–67

Ronda R J, de Bruin H A R and Holtslag A A M 2001 Representation of the canopy conductance in modeling the surface energy budget for low vegetation *J. Appl. Meteorol.* **40** 1431–44

Ross I, Misson L, Rambal S, Arneth A, Scott R L, Carrara A, Cescatti A and Genesio L 2012 How do variations in the temporal distribution of rainfall events affect ecosystem fluxes in seasonally water-limited Northern Hemisphere shrublands and forests? *Biogeosciences* **9** 1007–24

Saha S *et al* 2010 The NCEP climate forecast system reanalysis *Bull. Am. Meteorol. Soc.* **91** 1015–57

Sankaran M *et al* 2005 Determinants of woody cover in African savannas *Nature* **438** 846–9

Sato H 2009 Simulation of the vegetation structure and function in a Malaysian tropical rain forest using the individual-based dynamic vegetation model SEIB-DGVM *Forest Ecol. Manage.* **257** 2277–86

Sato H and Ise T 2012 Effect of plant dynamic processes on African vegetation responses to climate change: analysis using the spatially explicit individual-based dynamic global vegetation model (SEIB-DGVM) *J. Geophys. Res.* **117** G03017

Sato H, Itoh A and Kohyama T 2007 SEIB-DGVM: a new dynamic global vegetation model using a spatially explicit individual-based approach *Ecol. Modell.* **200** 279–307

Sato H, Kobayashi H and Delbart N 2010 Simulation study of the vegetation structure and function in eastern Siberian larch forests using the individual-based vegetation model SEIB-DGVM *Forest Ecol. Manage.* **259** 301–11

Schaffer B E, Nordbotten J M and Rodriguez-Iturbe I 2015 Plant biomass and soil moisture dynamics: analytical results *Proc. R. Soc. London A Math. Phys. Eng. Sci.* **471**

Seber G A F 1984 *Multivariate Observations* (Hoboken, NJ: Wiley)

Seth A, Rauscher S A, Biasutti M, Giannini A, Camargo S J and Rojas M 2013 CMIP5 projected changes in the annual cycle of precipitation in monsoon regions *J. Clim.* **26** 7328–51

Sheffield J, Goteti G and Wood E 2006 Development of a 50 year high-resolution global dataset of meteorological forcings for land surface modeling *J. Clim.* **19** 3088–111

Shongwe M E, van Oldenborgh G J, van den Hurk B J J M, de Boer B, Coelho C A S and van Aalst M K 2009 Projected changes in mean and extreme precipitation in Africa under global warming Part I: Southern Africa *J. Clim.* **22** 3819–37

Staver A C, Archibald S and Levin S 2011 Tree cover in sub-Saharan Africa: rainfall and fire constrain forest and savanna as alternative stable states *Ecology* **92** 1063–72

Strickland C, Liedloff A C, Cook G D, Dangelmayr G and Shipman P D 2016 The role of water and fire in driving tree dynamics in Australian savannas *J. Ecol.*

Thomey M L, Collins S L, Vargas R, Johnson J E, Brown R F, Natvig D O and Friggens M T 2011 Effect of precipitation variability on net primary production and soil respiration in a Chihuahuan Desert grassland *Glob. Change Biol.* **17** 1505–15

Trenberth K E, Dai A, Rasmussen R M and Parsons D B 2003 The changing character of precipitation *Bull. Am. Meteorol. Soc.* **84** 1205–17

Weltzin J *et al* 2003 Assessing the response of terrestrial ecosystems to potential changes in precipitation *Bioscience* **53** 941–52

Xu X, Medvigy D and Rodriguez-Iturbe I 2015 Relation between rainfall intensity and savanna tree abundance explained by water use strategies *Proc. Natl Acad. Sci.* **112** 12992–6

Xu X, Medvigy D, Trugman A, Guan K, Good S and Rodriguez-Iturbe I 2018 Tree cover shows strong sensitivity to precipitation variability across global tropics *Glob. Ecol. Biogeogr.* in preparation